Acta Virologica

TYPE Brief Research Report
PUBLISHED 12 October 2023
DOI 10.3389/av.2023.11782

OPEN ACCESS

EDITED BY
Miroslav Glasa,
Slovak Academy of Sciences, Slovakia

REVIEWED BY
Chrisa Orfanidou,
Aristotle University of Thessalonik, Greece
David Read,
University of Pretoria, South Africa

*CORRESPONDENCE
Yoonsoo Hahn,
hahny@cau.ac.kr

RECEIVED 08 July 2023
ACCEPTED 03 October 2023
PUBLISHED 12 October 2023

CITATION
Choi D, Rai M, Rai A, Yamazaki M and Hahn Y (2023), Discovery of two novel potyvirus genome sequences by high-throughput RNA sequencing in *Aconitum carmichaelii* tissue samples. *Acta Virol.* 67:11782.
doi: 10.3389/av.2023.11782

Discovery of two novel potyvirus genome sequences by high-throughput RNA sequencing in *Aconitum carmichaelii* tissue samples

Dongjin Choi[1], Megha Rai[2,3], Amit Rai[3,4], Mami Yamazaki[2,3] and Yoonsoo Hahn[1]*

[1]Department of Life Science, Chung-Ang University, Seoul, Republic of Korea, [2]Graduate School of Pharmaceutical Sciences, Chiba University, Chiba, Japan, [3]Plant Molecular Science Center, Chiba University, Chiba, Japan, [4]RIKEN Center for Sustainable Resource Science, Yokohama, Kanagawa, Japan

The genus *Potyvirus* (the family *Potyviridae*) is the largest group of plant-infecting viruses transmitted by aphids. Through high-throughput RNA sequencing analysis of asymptomatic samples of *Aconitum carmichaelii*, a significant medicinal herb in Asia, we identified the genome sequences of two RNA viruses, tentatively named Aconitum potyvirus 1 (AcoPV1) and Aconitum potyvirus 2 (AcoPV2). The genomes of AcoPV1 and AcoPV2 encode polyproteins composed of 3,069 and 3,054 amino acids, respectively. Sequence comparisons and phylogenetic analyses established that AcoPV1 and AcoPV2 represent unique, novel members within the genus *Potyvirus*. The estimated RNA polymerase slippage rates at the GAAAAAA motif, responsible for the production of P3N-PIPO or P3N-ALT trans-frame fusion proteins, were 0.79% in AcoPV1 and 1.38% in AcoPV2. The RNA reads of AcoPV1 and AcoPV2 were predominantly found in the leaf and flower tissues, indicating potential feeding preferences of vectors for these viruses. These findings demonstrate the effectiveness of high-throughput RNA sequencing in not only uncovering novel potyviruses, but also in elucidating their genomic dynamics within host plants.

KEYWORDS

Aconitum potyvirus 1, Aconitum potyvirus 2, polyprotein, PIPO, RNA polymerase slippage

Introduction

The genus *Potyvirus*, belonging to the family *Potyviridae*, represents the largest genus of plant viruses, containing 201 species approved by the International Committee on Taxonomy of Viruses[1] (last accessed 27 June, 2023) (Inoue-Nagata et al., 2022). Potyviruses have positive-sense single-stranded RNA genomes and

1 https://ictv.global/taxonomy

encode an open reading frame (ORF) for a large polyprotein. The potyvirus polyprotein is proteolytically processed to yield ten mature peptides, named P1 protease (P1), helper component-protease (HC-Pro), P3 protein (P3), 6-kilodalton (kDa) peptide 1 (6K1), cylindrical inclusion protein (CI), 6-kDa peptide 2 (6K2), viral protein genome-linked (VPg), nuclear inclusion-a protease (NIa-Pro), nuclear inclusion-b protein (NIb), and capsid protein (CP), in the sequence from N- to C-terminus (Goh and Hahn, 2021; Pasin et al., 2022). The viral protease P1, HC-Pro, and NIa-Pro recognize nine cleavage sites within the polyprotein: P1 and HC-Pro cleaves the P1/HC-Pro and HC-Pro/P3 junctions respectively, while NIa-Pro processes the other seven junctions (P3/6K1, 6K1/CI, CI/6K2, 6K2/VPg, VPg/NIa-Pro, NIa-Pro/NIb, and NIb/CP) (Adams et al., 2005a; Goh and Hahn, 2021). The NIb protein is an RNA-dependent RNA polymerase (RdRp) and plays a vital role in viral replication.

Potyviruses and other members of the family *Potyviridae* carry an additional small ORF, which is referred to as the pretty interesting Potyviridae ORF (PIPO) (Chung et al., 2008; Park et al., 2017; Choi et al., 2021). During the replication of the viral genome, the viral RdRp occasionally slips at a conserved sequence of GAAAAAA (GA_6) or a similar motif within the P3 coding region, leading to the insertion of an extra adenine (A) residue into the GA_6 sequence (Olspert et al., 2015; Rodamilans et al., 2015; Choi et al., 2021). The efficiency of the A residue insertion has been estimated to be between 0.8% and 2.1% in several potyviruses (Olspert et al., 2015; Rodamilans et al., 2015; Olspert et al., 2016; Untiveros et al., 2016). When these RNA polymerase slippage products are translated, a trans-frame fusion protein known as P3N-PIPO, which comprises the N-terminal region of P3 and a PIPO-derived peptide, is produced (Chung et al., 2008; Olspert et al., 2015). The P3N-PIPO protein plays a crucial role in facilitating the movement of potyvirus genomic RNAs from cell to cell (Wen and Hajimorad, 2010; Wang, 2021). An A residue can also be deleted from the GA_6 sequence, leading to the production of an alternative trans-frame fusion protein called P3N-ALT, which also plays a role in the movement of potyvirus genomic RNAs between cells (Hagiwara-Komoda et al., 2016).

Native plants are often associated with viruses that result in latent infections without exhibiting noticeable disease symptoms (Ilyas et al., 2022; Rosario et al., 2022; Cruz et al., 2023). The advent of high-throughput RNA sequencing (RNA-seq) has provided a tool for characterizing these viruses (Nibert et al., 2016; Bejerman and Debat, 2022). Numerous novel RNA virus genome sequences have been identified within assembled transcriptome contigs from diverse plant RNA-seq datasets (Goh et al., 2021; Park et al., 2021; Shin et al., 2022a; Shin et al., 2022b; Choi et al., 2022; Choi et al., 2023). In this study, we report discovery of two novel potyvirus genome sequences by high-throughput RNA-seq of *Aconitum carmichaelii* tissue samples.

Materials and methods

High-throughput RNA-seq data

In this study, we analyzed RNA-seq data originally collected from four tissue samples (flower, bud, leaf, and root) of a three-year-old *A. carmichaelii* plant with the aim of identifying key genes involved in the biosynthesis of diterpene alkaloids (Rai et al., 2017). The plant, which was cultivated under natural conditions at a research center in Tsukuba, Japan, did not show any symptoms of viral disease. The RNA-seq data are available in the Sequence Read Archive (SRA) of the National Center for Biotechnology Information (NCBI) under the accession numbers SRR6225420–SRR6225423. High-quality *A. carmichaelii* RNA-seq data were obtained by filtering raw data using sickle (version 1.33[2]) with the parameter "-q 30 -l 55." Transcriptome contigs were generated by assembling high-quality reads using the SPAdes Genome Assembler (version 3.15.4[3]) with the parameter "--rnaviral" (Bushmanova et al., 2019).

Viral genome identification and annotation

Putative viral genome contigs were initially identified by comparing *A. carmichaelii* transcriptome contigs with known viral RdRp domain sequences extracted from the Pfam database (release 35.0[4]) using DIAMOND (version v2.0.14.152[5]) (Buchfink et al., 2021). Accession numbers of the Pfam RdRp families used for preparation of known viral RdRp domains are PF00602, PF00603, PF00604, PF00680, PF00946, PF00972, PF00978, PF00998, PF02123, PF03431, PF04196, PF04197, PF05273, PF05788, PF05919, PF06317, PF06478, PF07925, PF08467, and PF12426. A polyprotein ORF of a putative potyvirus genome contig was predicted using the NCBI ORFfinder[6]. Protease cleavage sites of a polyprotein were identified by a sequence comparison with polyproteins of closely related viruses. Pairwise sequence identities were calculated using FASTA (version 36.3.8h[7]). Sequence logo representations were prepared using WebLogo (version 3[8]) (Schneider and Stephens, 1990; Crooks et al., 2004).

2 https://github.com/najoshi/sickle
3 https://github.com/ablab/spades
4 https://www.ebi.ac.uk/interpro/download/Pfam
5 https://github.com/bbuchfink/diamond
6 https://www.ncbi.nlm.nih.gov/orffinder
7 https://github.com/wrpearson/fasta36
8 http://weblogo.threeplusone.com

RNA polymerase slippage analysis

High-quality reads were mapped to potyviral genome contig sequences using BWA (version 0.7.17-r1194-dirty[9]) with the BWA-MEM algorithm (Li and Durbin, 2009). RNA-seq reads that span a putative RNA polymerase slippage site in the P3 coding region were extracted, and the frequency of insertions or deletions of A residues was determined.

Phylogenetic analysis

MAFFT (version 7.475[10]), with the parameter "--auto," was utilized for creating a multiple alignment of potyviral polyprotein sequences (Nakamura et al., 2018). Information-rich segments from the multiple sequence alignment were extracted using trimAl (version 1.4.rev22[11]) with the parameter "-automated1" (Capella-Gutierrez et al., 2009). The maximum likelihood phylogenetic tree was constructed using IQ-TREE (version 2.2.0[12]) with the "-B 1000" parameter (Minh et al., 2020). The resulting phylogenetic tree was visualized using MEGA (version 11.0.13[13]) (Kumar et al., 2018).

Results and discussion

Identification of novel potyvirus genomes

RNA-seq reads previously generated from four tissue types (flower, bud, leaf, and root) of a three-year-old *A. carmichaelii* plant were assembled into contigs (Rai et al., 2017). Two of these contigs, with lengths of 9,492 and 9,441 bp respectively, exhibited significant sequence similarities to RdRp sequences of known potyviruses. They contained a full-length coding region for potyviral polyproteins, although the completeness of the genomes should be verified through a molecular method such as rapid amplification of cDNA ends. The predicted polyprotein ORFs had lengths of 9,210 and 9,165 bp, encoding 3,069 and 3,054 aa polyproteins, respectively.

BLAST searches of the NCBI protein database revealed that the two putative potyvirus genome contigs identified in the *A. carmichaelii* transcriptome were most similar to tulip breaking virus (TBV), a member of the genus Potyvirus, with approximately 56% amino acid sequence identity of polyprotein sequences (Wylie et al., 2019). The species demarcation criteria for potyviruses are generally accepted as <76% nucleotide identity of the large ORF and <82% amino acid identity of the polyprotein (Adams et al., 2005b; Inoue-Nagata et al., 2022). Therefore, the two newly identified viruses can be considered novel and distinct from previously known potyviruses. The second most closely related known potyvirus was lily mottle virus (LMoV), with around 53% amino acid sequence identity of polyprotein sequences (Zheng et al., 2003).

The polyprotein ORFs of the two newly identified potyvirus genome contigs exhibited a nucleotide sequence identity of 66%, while the amino acid sequence identity of polyprotein sequences was 69%. According to the aforementioned demarcation criteria, the two genome sequences were considered to originate from distinct potyviruses and were tentatively named Aconitum potyvirus 1 (AcoPV1, 9,492 bp) and Aconitum potyvirus 2 (AcoPV2, 9,441 bp). The AcoPV1 and AcoPV2 sequences were deposited in the NCBI GenBank under accession numbers OP271473 and OP271474, respectively.

The large polyprotein of a potyvirus is processed into ten mature peptides (P1, HC-Pro, P3, 6K1, CI, 6K2, VPg, NIa-Pro, NIb, and CP) by the three potyvirus proteases (P1, HC-Pro, and NIa-Pro) (Adams et al., 2005a; Goh and Hahn, 2021; Pasin et al., 2022). Cleavage sites and boundaries of mature peptides were predicted in the AcoPV1 and AcoPV2 polyproteins based on sequence similarities with mature proteins of closely related potyviruses, including TBV and LMoV (Figure 1). The polyprotein sequences of AcoPV1 and AcoPV2 surrounding the cleavage sites matched previously deduced consensus sequences for the potyvirus protease recognition sites (Adams et al., 2005a; Goh and Hahn, 2021).

All members of the family *Potyviridae* are known to have a secondary ORF, termed PIPO, which is situated in the P3 coding region, and is in frame −1 relative to the P3 (Yang et al., 2021; Inoue-Nagata et al., 2022). The PIPO ORF is expressed into a trans-frame fusion protein, known as P3N-PIPO, due to the insertion of an A residue at the slippery GA_6 motif during replication (Chung et al., 2008). In the genomes of AcoPV1 and AcoPV2, the GA_6 motifs were located at positions 2,802–2,808 and 2,782–2,788, respectively. The PIPO ORFs of AcoPV1 and AcoPV2 encode 59 and 82 amino acids, respectively. No additional GA_6 motif other than that in the P3 coding region was found in AcoPV1 and AcoPV2 sequences.

RNA polymerase slippages of AcoPV1 and AcoPV2

The GA_6 motif within the P3 coding region of potyviruses induces rare RNA polymerase slippages during replication, resulting in the crucial insertion of an A residue for P3N-PIPO protein production (Olspert et al., 2015; Rodamilans et al., 2015; Hagiwara-Komoda et al., 2016; Olspert et al.,

9 https://github.com/lh3/bwa

10 https://mafft.cbrc.jp/alignment/software

11 http://trimal.cgenomics.org

12 http://www.iqtree.org

13 https://www.megasoftware.net

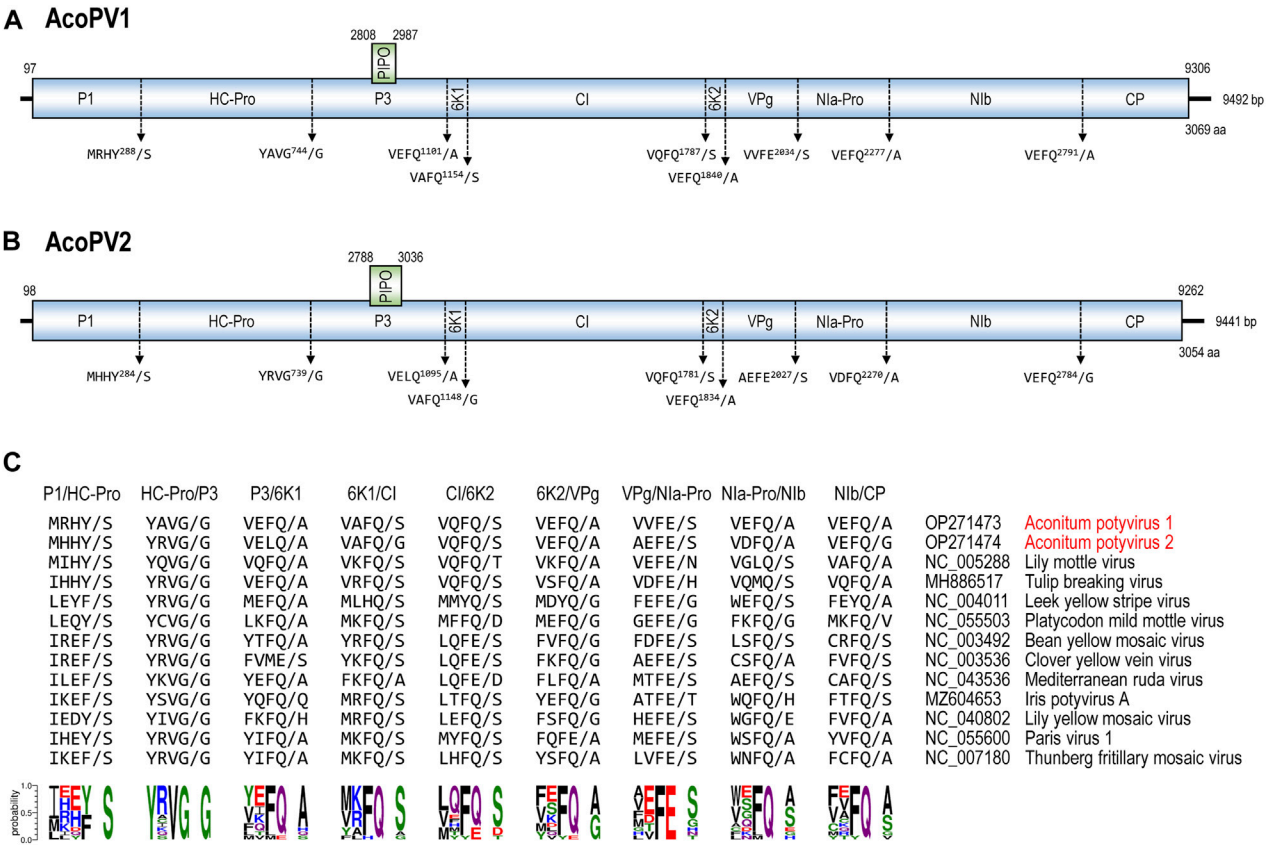

FIGURE 1
The genomic structure of AcoPV1 and AcoPV2. **(A, B)** The diagrams illustrate the genomic contigs of AcoPV1 **(A)** and AcoPV2 **(B)**. The ORFs for the large polyprotein and PIPO are depicted as boxes, with their coordinates indicated above. Predicted cleavage sites are displayed below the polyprotein, with the slash ("/") marking the cleaved bond. **(C)** The five amino acid residues at the nine cleavage sites of the AcoPV1, AcoPV2, and 11 closely related potyvirus polyprotein sequences are presented. At the bottom, sequence logo representations derived from the frequency of each amino acid residue at each position are shown.

2016; Untiveros et al., 2016). The RNA polymerase slippage rate can be estimated by counting RNA-seq reads originating from the slippage products in the GA_6 motif. To detect and quantify the slippage products of the AcoPV1 and AcoPV2, RNA-seq reads spanning the GA_6 motifs were extracted and examined (Figure 2).

A total of 509 and 1,084 RNA-seq reads were mapped to the GA_6 motif in AcoPV1 and AcoPV2, respectively. Among these, 505 (99.21%) for AcoPV1 and 1,069 (98.62%) for AcoPV2 matched the original unmodified (wild type) sequence. There was one read for AcoPV1 (0.20%) and seven reads for AcoPV2 (0.65%) that potentially originated from the single-A insertion or +1A product, which is essential for P3N-PIPO protein production.

Interestingly, we also observed RNA-seq reads corresponding to other insertion or deletion products. One of these slippage products, the single-A deletion or −1A product, might lead to the production of another trans-frame fusion protein, known as P3N-ALT, as previously reported in clover yellow vein virus (ClYVV) (Hagiwara-Komoda et al., 2016). In AcoPV1, one read (0.20%) was identified as the −1A product, potentially encoding P3N-ALT, if present. The −1A product in AcoPV1 results in the addition of 12 amino acids after the GA_6 motif. In the case of AcoPV2, four reads (0.37%) were identified as the −1A product, which could add five amino acids after the GA_6 motif. Additionally, we also observed other slippage products, including double-A deletion (−2A) or double-A insertion (+2A) products. These slippage products may be translated to produce P3N-ALT with a single amino acid deletion or P3N-PIPO with a single amino acid insertion, respectively.

As a result, we estimated the rate of RNA polymerase slippage, potentially leading to the production of P3N-PIPO or P3N-ALT, to be 0.79% in AcoPV1 and 1.38% in AcoPV2. It is worth noting that the number of RNA-seq reads originating from slippage products is too low to accurately measure their RNA polymerase slippage rates.

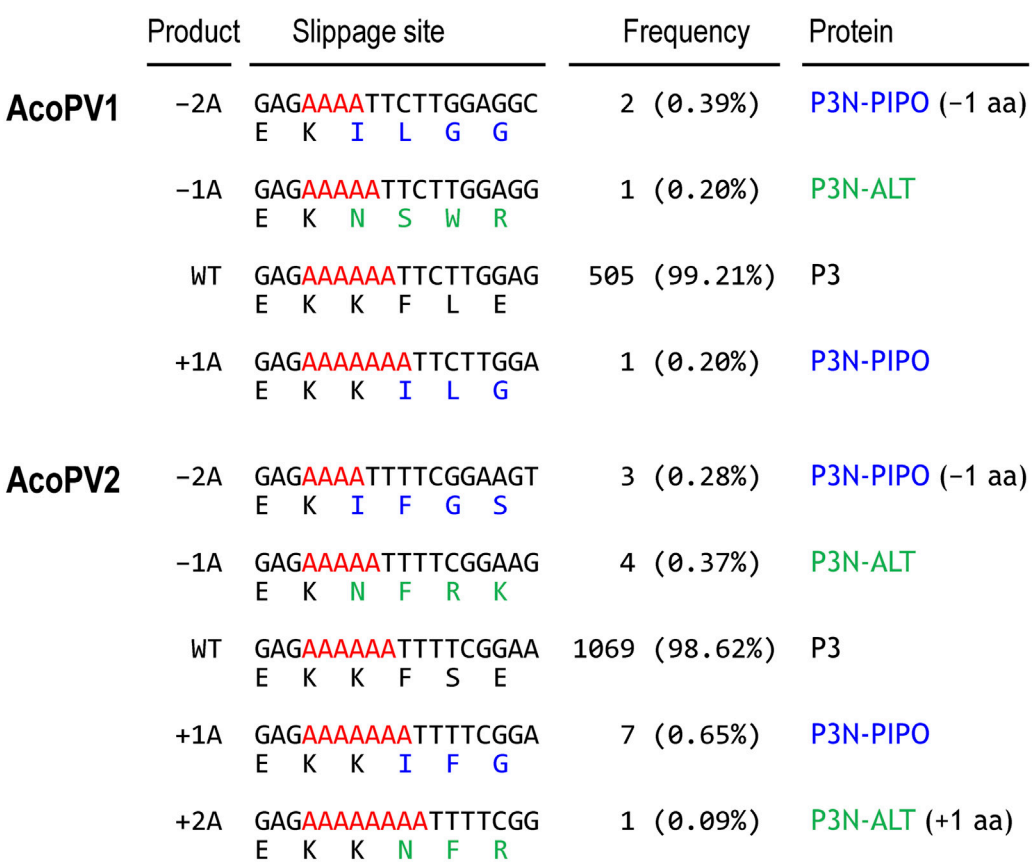

FIGURE 2
RNA polymerase slippages at the GA_6 motif. Frequencies of slippage products generated by potential RNA polymerase slippage events in the AcoPV1 (top) and AcoPV2 (bottom) are presented. These slippage products include double-A deletion (−2A), single-A deletion (−1A), single-A insertion (+1A), and double-A insertion (+2A), compared to the wild type (WT). Adenine residues of the GA_6 motif are highlighted in red. Amino acid sequences are color-coded to indicate residues from frame 0 (black, P3), frame −1 (blue, P3N-PIPO), and frame +1 (green, P3N-ALT).

Phylogenetic positions of AcoPV1 and AcoPV2

To determine the phylogenetic positions of AcoPV1 and AcoPV2 among known potyviruses, we retrieved polyprotein sequences of known potyviruses from the NCBI protein database. The pairwise identities of polyprotein sequences of AcoPV1, AcoPV2, and other potyviruses are presented in Supplementary Table S1. A maximum likelihood phylogenetic tree was inferred from a multiple sequence alignment that included AcoPV1, AcoPV2, and known polyprotein sequences (Figure 3).

Both AcoPV1 and AcoPV2 cluster together into a subclade, supported by a 100% bootstrap value, distinct from the known potyviruses. The clade that includes TBV and LMoV is the most closely related known potyvirus group to AcoPV1 and AcoPV2. Together, the AcoPV1/AcoPV2 and TBV/LMoV subclades form a single clade, supported by a 99% bootstrap value (green box in Figure 3).

The next most closely related clade comprises nine potyviruses: leek yellow stripe virus, Platycodon mild mottle virus, bean yellow mosaic virus, ClYVV, Mediterranean ruda virus, iris potyvirus A, lily yellow mosaic virus, Paris virus 1, and Thunberg fritillary mosaic virus. AcoPV1, AcoPV2, TBV, LMoV, and these nine potyviruses form a robust clade within the genus *Potyvirus*, supported by a 100% bootstrap value (blue box in Figure 3).

Abundance and distribution of AcoPV1 and AcoPV2 in *A. carmichaelii* tissues

Potyviruses are primarily transmitted by aphids, which feed on sap from leaves and other easily accessible parts of host plants (Gadhave et al., 2020; Xia et al., 2023). To assess the distribution and abundance of AcoPV1 and AcoPV2 within *A. carmichaelii* tissue samples, we counted all mapped RNA-seq reads to the viral genome sequences (Table 1).

In flower and leaf tissues, the viral RNA-seq reads of AcoPV1 and AcoPV2 were notably higher compared to bud and root tissues. In the flower tissue, AcoPV1 and AcoPV2 viral

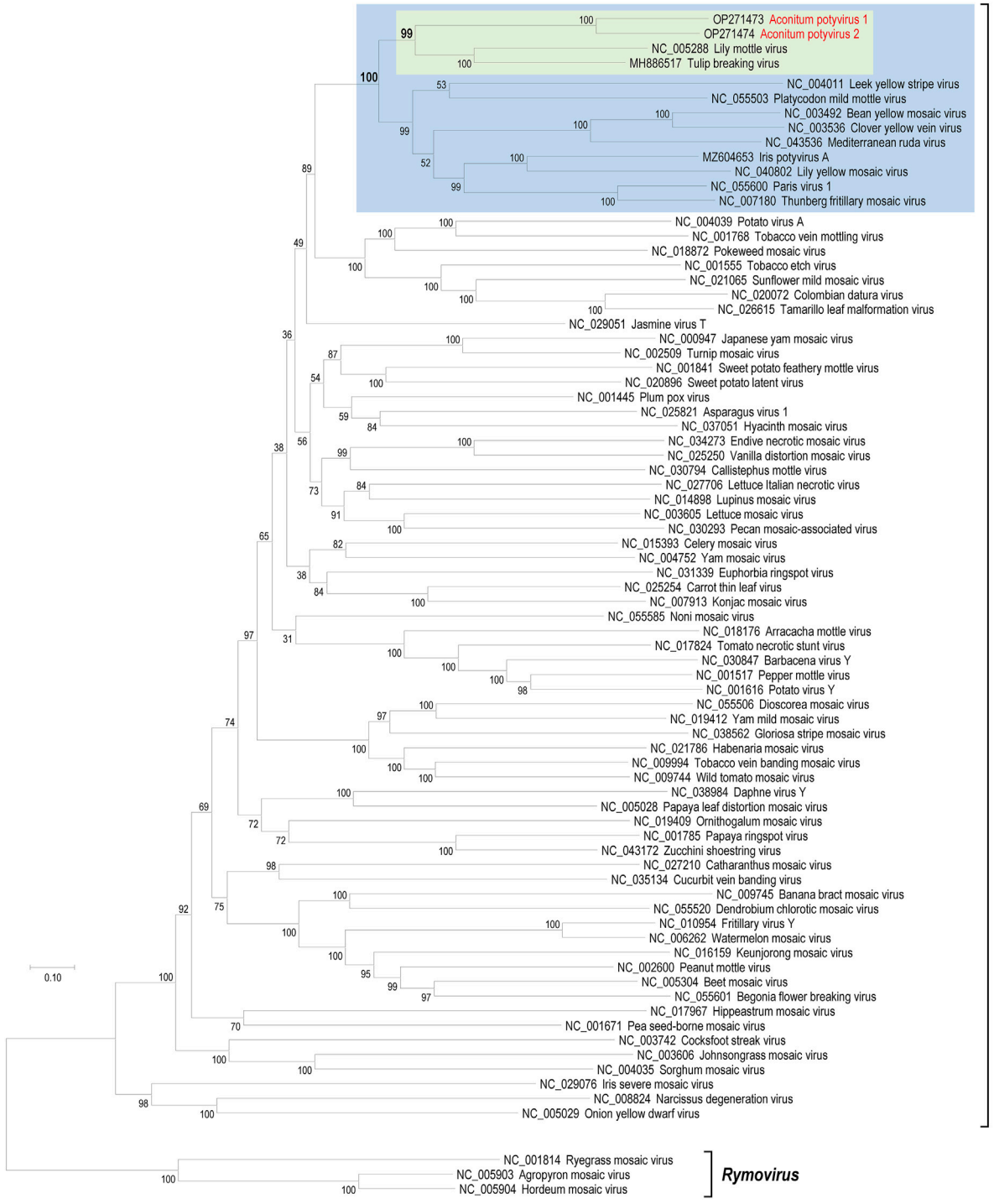

FIGURE 3
Phylogenetic positions of AcoPV1 and AcoPV2. The maximum likelihood phylogenetic tree was inferred from multiple alignment of selected potyvirus polyprotein sequences. The potyviruses most similar to AcoPV1 and AcoPV2 were lily mottle virus (LMoV) and tulip breaking virus (TBV), which are highlighted in the green box. AcoPV1, AcoPV2, LMoV, TBV, and other nine potyviruses formed a strong subclade, marked with a blue box, within the genus *Potyvirus*. The genus *Rymovirus*, represented by three rymoviruses, was used as an outgroup to root the genus *Potyvirus*.

TABLE 1 Virus-derived reads in the *A. carmichaelii* samples.

Sample	SRA accession	Total[a]	AcoPV1[b]	AcoPV2[b]
Flower	SRR6225420	8,643,220	18,977 (0.22%)	75,657 (0.88%)
Bud	SRR6225421	8,212,299	1,680 (0.02%)	14,782 (0.18%)
Leaf	SRR6225422	6,301,821	44,359 (0.70%)	22,450 (0.36%)
Root	SRR6225423	5,662,020	2 (<0.01%)	12 (<0.01%)

[a]Total high-quality reads.
[b]Number and percentage of mapped reads.

reads accounted for 0.22% and 0.88%, respectively, of the total RNA-seq reads. In leaf tissue, viral reads corresponding to the AcoPV1 and AcoPV2 genomes comprised 0.70% and 0.36%, respectively. For bud tissue, we observed lower quantities, with 0.02% for AcoPV1 and 0.18% for AcoPV2. In root tissue, both viruses showed the lowest counts among tissues studied (less than 0.01%).

It is notable that the *A. carmichaelii* plant analyzed in this study did not display any viral disease symptoms. This suggests that viral infection may be at an initial stage, and their distribution may be limited to the original infection site or nearby tissues. Consequently, the higher abundance of AcoPV1 and AcoPV2 RNA-seq reads in leaf and flower tissues may reflect the feeding preferences of aphids, which are likely their primary vectors.

Data availability statement

The datasets presented in this study can be found in online repositories. The names of the repository/repositories and accession number(s) can be found below: https://www.ncbi.nlm.nih.gov/genbank/, OP271473, OP271474.

Author contributions

MR, AR, and MY obtained RNA-seq data; DC and YH performed bioinformatics analysis; YH wrote the manuscript. All authors contributed to the article and approved the submitted version.

Funding

This work was supported by National Research Foundation of Korea (NRF) grants funded by the Government of Korea (grant numbers 2018R1A5A1025077 and RS-2023-00208564).

Conflict of interest

The authors declare that the research was conducted in the absence of any commercial or financial relationships that could be construed as a potential conflict of interest.

Supplementary material

The Supplementary Material for this article can be found online at: https://www.frontierspartnerships.org/articles/10.3389/av.2023.11782/full#supplementary-material

References

Adams, M. J., Antoniw, J. F., and Beaudoin, F. (2005a). Overview and analysis of the polyprotein cleavage sites in the family *potyviridae*. *Mol. Plant Pathol.* 6, 471–487. doi:10.1111/j.1364-3703.2005.00296.x

Adams, M. J., Antoniw, J. F., and Fauquet, C. M. (2005b). Molecular criteria for genus and species discrimination within the family *potyviridae*. *Arch. Virol.* 150, 459–479. doi:10.1007/s00705-004-0440-6

Bejerman, N., and Debat, H. (2022). Exploring the *tymovirales* landscape through metatranscriptomics data. *Arch. Virol.* 167, 1785–1803. doi:10.1007/s00705-022-05493-9

Buchfink, B., Reuter, K., and Drost, H. G. (2021). Sensitive protein alignments at tree-of-life scale using DIAMOND. *Nat. Methods* 18, 366–368. doi:10.1038/s41592-021-01101-x

Bushmanova, E., Antipov, D., Lapidus, A., and Prjibelski, A. D. (2019). rnaSPAdes: a *de novo* transcriptome assembler and its application to RNA-seq data. *GigaScience* 8, giz100. doi:10.1093/gigascience/giz100

Capella-Gutierrez, S., Silla-Martinez, J. M., and Gabaldon, T. (2009). trimAl: a tool for automated alignment trimming in large-scale phylogenetic analyses. *Bioinformatics* 25, 1972–1973. doi:10.1093/bioinformatics/btp348

Choi, D., Shin, C., Shirasu, K., Ichihashi, Y., and Hahn, Y. (2022). Artemisia capillaris nucleorhabdovirus 1, a novel member of the genus *alphanucleorhabdovirus*, identified in the *artemisia capillaris* transcriptome. *Acta Virol.* 66, 149–156. doi:10.4149/av_2022_204

Choi, D., Rai, M., Rai, A., Shin, C., Yamazaki, M., and Hahn, Y. (2023). High-throughput RNA sequencing analysis of *mallotus japonicus* revealed novel polerovirus and amalgavirus. *Acta Virol.* 67, 13–23. doi:10.4149/av_2023_102

Choi, D., Shin, C., Shirasu, K., and Hahn, Y. (2021). Two novel poty-like viruses identified from the transcriptome data of purple witchweed (*Striga hermonthica*). *Acta Virol.* 65, 365–372. doi:10.4149/av_2021_402

Chung, B. Y., Miller, W. A., Atkins, J. F., and Firth, A. E. (2008). An overlapping essential gene in the *potyviridae*. *Proc. Natl. Acad. Sci. U. S. A.* 105, 5897–5902. doi:10.1073/pnas.0800468105

Crooks, G. E., Hon, G., Chandonia, J. M., and Brenner, S. E. (2004). WebLogo: a sequence logo generator: figure 1. *Genome Res.* 14, 1188–1190. doi:10.1101/gr.849004

Cruz, J. A., Freire, A. M., Polimeni, J. C., and Blawid, R. (2023). A novel deltacryptic virus identified in *allium cepa* from Brazil. *Acta Virol.* 67, 109–113. doi:10.4149/av_2023_111

Gadhave, K. R., Gautam, S., Rasmussen, D. A., and Srinivasan, R. (2020). Aphid transmission of *potyvirus*: the largest plant-infecting RNA virus genus. *Viruses* 12, 773. doi:10.3390/v12070773

Goh, C. J., and Hahn, Y. (2021). Analysis of proteolytic processing sites in potyvirus polyproteins revealed differential amino acid preferences of NIa-Pro protease in each of seven cleavage sites. *PLoS One* 16, e0245853. doi:10.1371/journal.pone.0245853

Goh, C. J., Park, D., and Hahn, Y. (2021). A novel tepovirus, agave virus T, identified by the analysis of the transcriptome data of blue agave (*Agave tequilana*). *Acta Virol.* 65, 68–71. doi:10.4149/av_2021_107

Hagiwara-Komoda, Y., Choi, S. H., Sato, M., Atsumi, G., Abe, J., Fukuda, J., et al. (2016). Truncated yet functional viral protein produced via RNA polymerase slippage implies underestimated coding capacity of RNA viruses. *Sci. Rep.* 6, 21411. doi:10.1038/srep21411

Ilyas, R., Rohde, M. J., Richert-Poggeler, K. R., and Ziebell, H. (2022). To be seen or not to be seen: latent infection by tobamoviruses. *Plants (Basel)* 11, 2166. doi:10.3390/plants11162166

Inoue-Nagata, A. K., Jordan, R., Kreuze, J., Li, F., Lopez-Moya, J. J., Makinen, K., et al. (2022). ICTV virus taxonomy profile: *potyviridae* 2022. *J. Gen. Virol.* 103, 001738. doi:10.1099/jgv.0.001738

Kumar, S., Stecher, G., Li, M., Knyaz, C., and Tamura, K. (2018). MEGA X: molecular evolutionary genetics analysis across computing platforms. *Mol. Biol. Evol.* 35, 1547–1549. doi:10.1093/molbev/msy096

Li, H., and Durbin, R. (2009). Fast and accurate short read alignment with burrows-wheeler transform. *Bioinformatics* 25, 1754–1760. doi:10.1093/bioinformatics/btp324

Minh, B. Q., Schmidt, H. A., Chernomor, O., Schrempf, D., Woodhams, M. D., von Haeseler, A., et al. (2020). IQ-TREE 2: new models and efficient methods for phylogenetic inference in the genomic era. *Mol. Biol. Evol.* 37, 1530–1534. doi:10.1093/molbev/msaa015

Nakamura, T., Yamada, K. D., Tomii, K., and Katoh, K. (2018). Parallelization of MAFFT for large-scale multiple sequence alignments. *Bioinformatics* 34, 2490–2492. doi:10.1093/bioinformatics/bty121

Nibert, M. L., Pyle, J. D., and Firth, A. E. (2016). A +1 ribosomal frameshifting motif prevalent among plant amalgaviruses. *Virology* 498, 201–208. doi:10.1016/j.virol.2016.07.002

Olspert, A., Carr, J. P., and Firth, A. E. (2016). Mutational analysis of the *potyviridae* transcriptional slippage site utilized for expression of the P3N-PIPO and P1N-PISPO proteins. *Nucleic Acids Res.* 44, 7618–7629. doi:10.1093/nar/gkw441

Olspert, A., Chung, B. Y., Atkins, J. F., Carr, J. P., and Firth, A. E. (2015). Transcriptional slippage in the positive-sense RNA virus family potyviridae. *EMBO Rep.* 16, 995–1004. doi:10.15252/embr.201540509

Park, D., Goh, C. J., and Hahn, Y. (2021). Two novel closteroviruses, fig virus A and fig virus B, identified by the analysis of the high-throughput RNA-sequencing data of fig (*Ficus carica*) latex. *Acta Virol.* 65, 42–48. doi:10.4149/av_2021_104

Park, D., Kim, H., and Hahn, Y. (2017). Genome sequence of a distinct watermelon mosaic virus identified from ginseng (*Panax ginseng*) transcriptome. *Acta Virol.* 61, 479–482. doi:10.4149/av_2017_410

Pasin, F., Daros, J. A., and Tzanetakis, I. E. (2022). Proteome expansion in the *potyviridae* evolutionary radiation. *FEMS Microbiol. Rev.* 46, fuac011. doi:10.1093/femsre/fuac011

Rai, M., Rai, A., Kawano, N., Yoshimatsu, K., Takahashi, H., Suzuki, H., et al. (2017). *De novo* RNA sequencing and expression analysis of *aconitum carmichaelii* to analyze key genes involved in the biosynthesis of diterpene alkaloids. *Molecules* 22, 2155. doi:10.3390/molecules22122155

Rodamilans, B., Valli, A., Mingot, A., San Leon, D., Baulcombe, D., Lopez-Moya, J. J., et al. (2015). RNA polymerase slippage as a mechanism for the production of frameshift gene products in plant viruses of the *potyviridae* family. *J. Virol.* 89, 6965–6967. doi:10.1128/JVI.00337-15

Rosario, K., Van Bogaert, N., Lopez-Figueroa, N. B., Paliogiannis, H., Kerr, M., and Breitbart, M. (2022). Freshwater macrophytes harbor viruses representing all five major phyla of the RNA viral kingdom *orthornavirae*. *PeerJ* 10, e13875. doi:10.7717/peerj.13875

Schneider, T. D., and Stephens, R. M. (1990). Sequence logos: a new way to display consensus sequences. *Nucleic Acids Res.* 18, 6097–6100. doi:10.1093/nar/18.20.6097

Shin, C., Choi, D., Shirasu, K., and Hahn, Y. (2022a). Identification of dicistro-like viruses in the transcriptome data of *striga asiatica* and other plants. *Acta Virol.* 66, 157–165. doi:10.4149/av_2022_205

Shin, C., Choi, D., Shirasu, K., Ichihashi, Y., and Hahn, Y. (2022b). A novel RNA virus, thesium chinense closterovirus 1, identified by high-throughput RNA-sequencing of the parasitic plant *thesium chinense*. *Acta Virol.* 66, 206–215. doi:10.4149/av_2022_302

Untiveros, M., Olspert, A., Artola, K., Firth, A. E., Kreuze, J. F., and Valkonen, J. P. (2016). A novel sweet potato potyvirus open reading frame (ORF) is expressed via polymerase slippage and suppresses RNA silencing. *Mol. Plant Pathol.* 17, 1111–1123. doi:10.1111/mpp.12366

Wang, A. (2021). Cell-to-cell movement of plant viruses via plasmodesmata: a current perspective on potyviruses. *Curr. Opin. Virol.* 48, 10–16. doi:10.1016/j.coviro.2021.03.002

Wen, R. H., and Hajimorad, M. R. (2010). Mutational analysis of the putative pipo of soybean mosaic virus suggests disruption of PIPO protein impedes movement. *Virology* 400, 1–7. doi:10.1016/j.virol.2010.01.022

Wylie, S. J., Tran, T. T., Nguyen, D. Q., Koh, S. H., Chakraborty, A., Xu, W., et al. (2019). A virome from ornamental flowers in an australian rural town. *Arch. Virol.* 164, 2255–2263. doi:10.1007/s00705-019-04317-7

Xia, C. C., Xue, W. J., Li, Z. Z., Shi, J. X., Yu, G. F., and Zhang, Y. (2023). Presenting the secrets: exploring endogenous defense mechanisms in chrysanthemums against aphids. *Horticulturae* 9, 937. doi:10.3390/horticulturae9080937

Yang, X., Li, Y., and Wang, A. (2021). Research advances in potyviruses: from the laboratory bench to the field. *Annu. Rev. Phytopathol.* 59, 1–29. doi:10.1146/annurev-phyto-020620-114550

Zheng, H. Y., Chen, J., Zhao, M. F., Lin, L., Chen, J. P., Antoniw, J. F., et al. (2003). Occurrence and sequences of lily mottle virus and lily symptomless virus in plants grown from imported bulbs in Zhejiang province, China. *Arch. Virol.* 148, 2419–2428. doi:10.1007/s00705-003-0207-5